

Monte Carlo analysis of four-terminal ballistic rectifiers

B G Vasallo, T González, D Pardo and J Mateos

Departamento de Física Aplicada, Universidad de Salamanca, Plaza de la Merced s/n, 37008, Salamanca, Spain

E-mail: a50343@usal.es

Received 6 October 2003

Published 27 February 2004

Online at stacks.iop.org/Nano/15/S250 (DOI: 10.1088/0957-4484/15/4/025)

Abstract

We present a Monte Carlo study of an InGaAs based four-terminal ballistic rectifier operating at different temperatures. The rectifying effect is due to the vertical asymmetry of the electron concentration originated, in the presence of ballistic transport, by the action of an obstacle located in the centre of a ballistic cross junction. An increase of temperature degrades the efficiency of the device, since transport becomes more diffusive. However, it shows an intrinsic capability for rectification up to a frequency of 1.0 THz almost independently of the temperature.

1. Introduction

The use of devices exploiting ballistic transport of electrons is a possible approach for overcoming the limits of traditional scaling when reaching the nanometre range. Indeed, recent works have achieved an important improvement of this type of device using InGaAs channels with high In content [1, 2], for which room temperature operation is possible, since the mean free path of electrons in this material is still larger than 100 nm at 300 K. Moreover, InGaAs based ballistic devices offer the advantage of being compatible with modern HEMT technology. In particular, novel semiconductor rectifiers based on ballistic electron transport have been fabricated by inserting a triangular scatterer (antidot) into the centre of a ballistic cross junction [3, 4].

The design cycle for ballistic structures can be considerably accelerated by using simulation tools for the determination of the optimal geometry of the devices; this represents a helpful alternative to the expensive and time-consuming trial-and-error procedure. In this work we present a microscopic study, performed by means of Monte Carlo (MC) simulations, of the transport properties and the dynamic behaviour of a ballistic rectifier with a similar geometry to that studied in [4], based on AlInAs/InGaAs channels. MC simulations, based on a semiclassical transport description, provide insight into the processes taking place inside the devices, thus allowing us to relate the macroscopic results of the experiments to the microscopic behaviour of electrons. Our model is able to qualitatively reproduce the main features of the ballistic effects measured in actual devices (particularly in

real rectifiers) [5, 6], thus indicating that coherent transport plays no significant role in the main characteristics of these devices. Moreover, due to the versatility of the MC method, our approach allows us to analyse and optimize different possible geometries for the ballistic rectifier and to study its behaviour at different temperatures.

In section 2, the details of the MC model and the simulated device are given and in section 3, results from the MC simulation concerning the static and dynamic behaviour of the ballistic rectifier are presented. Finally, in section 4 we draw the most important conclusions of our work.

2. Physical model

We make use of a semiclassical ensemble MC simulator, which includes all the details of scattering mechanisms, self-consistently coupled with a 2D Poisson solver. The validity of our approach has been checked in previous works by obtaining favourable comparisons with experimental results on static characteristics, small signal behaviour and noise performance of InP based δ -doped 100 nm T-gate AlInAs/InGaAs lattice match HEMTs (InP based) [6]. Since the contact injection is a critical point when dealing with ballistic transport, the velocity distribution and time characteristics of injected carriers at the left and right branches are accurately modelled following [7].

The device under analysis consists of a ballistic cross junction, in whose centre a triangular scatterer (antidot) has been inserted, as shown in the inset of figure 1. The top and bottom branches remain open-circuited. For the exact analysis of these devices, a 3D simulation would be necessary

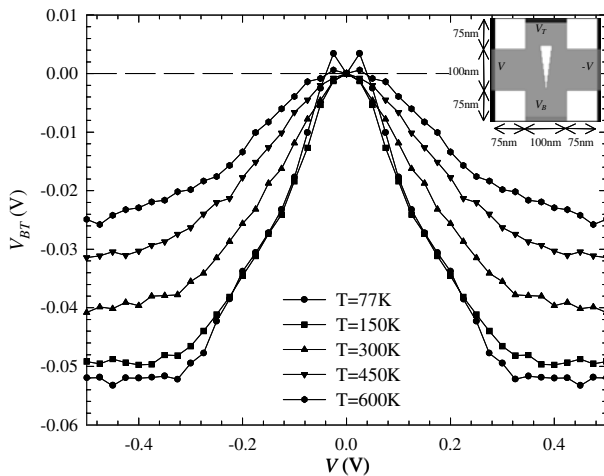


Figure 1. Potential difference between the bottom and top branches, V_{BT} , as a function of V when biasing with $V = V_L = -V_R$ the left and right branches of the ballistic rectifier with the geometry shown in the inset, at different temperatures.

in order to consider the effect of the lateral surface charges and the real layer structure. When using 2D simulations some simplifications must be made. We perform a top view simulation of the device, where the real layer structure is not included and only the channel is simulated [6]. To consider the positive charges of the whole layer structure, a net background doping is assigned to the channel, but impurity scattering is switched off. Thus, the electron transport through the undoped channel is well reproduced, since this is a ‘virtual’ doping associated with the charges of the cap and δ -doping layers. In addition, a negative surface charge density is assigned to the semiconductor–air interfaces to account for the influence of the surface states originated by the etching processes. Therefore, the values of three important parameters must be carefully chosen: the effective doping of the injecting contacts, N_C , the background doping of the channel, N_{Db} , and the lateral surface charge density, σ . We consider $N_C = 4 \times 10^{17} \text{ cm}^{-3}$, $N_{Db} = 10^{17} \text{ cm}^{-3}$ and $\sigma = 0.25 \times 10^{12} \text{ cm}^{-2}$. For these values, a reasonable agreement with experiments in ballistic channels has been found [5, 6]. More details of the model can be found in [6].

3. Results

Figure 1 shows the values of the potential difference between the bottom and the top branches of the device, $V_{BT} = V_B - V_T$, obtained from the MC simulation of the ballistic rectifier sketched in the inset at several temperatures when biasing left and right branches in push–pull fashion, $V = V_L = -V_R$. For these biasing conditions, a negative potential appears in both central branches (bottom and top), but with different values due to the unequal widths of the opening space between the horizontal and the top/bottom branches, leading to an asymmetric injection of carriers into them. This effect appears starting from the lowest applied potentials, since all the openings are conductive even at equilibrium conditions (i.e., leading to bias dependent transmission coefficients within the formalism of [8, 9]). The curvature of V_B as a function of V is higher than that of V_T [6]; thus negative values for V_{BT} are

obtained. The behaviour of V_{BT} for low V remains parabolic up to a given biasing, for which the unbalanced injection of charge into the top and bottom branches reaches a saturation regime and V_{BT} takes a constant value. The origin of the rectifying effect can be understood as a consequence of the horizontal asymmetry of the electron concentration associated with both the ballistic transport and the space charge inside the device, and the different openings between the horizontal and top/bottom branches [6]. Thus, since this behaviour is due to the ballistic transport of electrons through the device, for the lowest temperatures (77 and 150 K), the rectifying effect is more significant (higher absolute values of V_{BT}) than at higher temperatures. At the same time, the results for 77 and 150 K are very similar, thus indicating that at both temperatures transport is practically ballistic. In contrast, the rectifying effect is less pronounced when increasing the temperature above 300 K. In these cases, transport in the structures approaches the diffusive regime, thus reducing the influence of the asymmetric shape of the scatterer on the injection of carriers into the top/bottom branches. In the case of purely diffusive transport the effect should disappear, since the device would be completely symmetric in the horizontal direction (the resistance between a given vertical branch and both horizontal branches would be the same). At 300 K the transport is still quasi-ballistic, so the ballistic rectifier can be used for room temperature operation.

In order to analyse the dynamic behaviour of the ballistic rectifier, figure 2 shows the V_{BT} response to periodic AC signals, $V_{LR}(t)$, with the amplitude of 0.2 V and frequencies of 200 GHz, 1.0 and 3.0 THz applied between the left and right electrodes at different temperatures. We have chosen this amplitude in order for the applied signal to remain inside the linear part of the static characteristic $V_{BT} - V_{LR}$ (figure 1). Figures 2(a)–(f) correspond to operation at 300 K and figures 2(g)–(l), to operation at 77 K. Figures 2(a)–(c) and (g)–(i) present the applied AC input signals, and the horizontal current flowing from the left to the right electrodes normalized to the maximum current, I_{LR}/I_{max} . On the other hand, figures 2(d)–(f) and (j)–(l) show the time dependent vertical response, $V_{BT}(t)$, together with its mean value, $\overline{V_{BT}}$. When the operation frequency is 200 GHz, for both temperatures 300 and 77 K the device response can be considered as quasi-static; $V_{BT}(t)$ takes the DC value shown in figure 1 for the corresponding $V_{LR}(t)$, thus showing a higher efficiency at 77 K than at 300 K. If the frequency of the input signal is increased to 1.0 THz, even if the mean value of the response, $\overline{V_{BT}}$, decreases, the amplitude of $V_{BT}(t)$ is higher than at low frequency. Moreover, a delay between the input and output signals can be detected and $V_{BT}(t)$ can even take positive values. If we further increase the input frequency to 3.0 THz, the amplitude of the response signal decreases significantly (indeed, the frequency-doubling action of the device disappears completely) and, remarkably, $\overline{V_{BT}}$ takes positive values. This high frequency behaviour occurs due to an overshoot in the current through the device; this is possibly related to the fact that when the transit time of the electrons is longer than the period of the signal, electrons do not have enough time to complete the path between the left and right electrodes, but only a part of it. However, it is necessary that they arrive to the bottom and top branches to provide

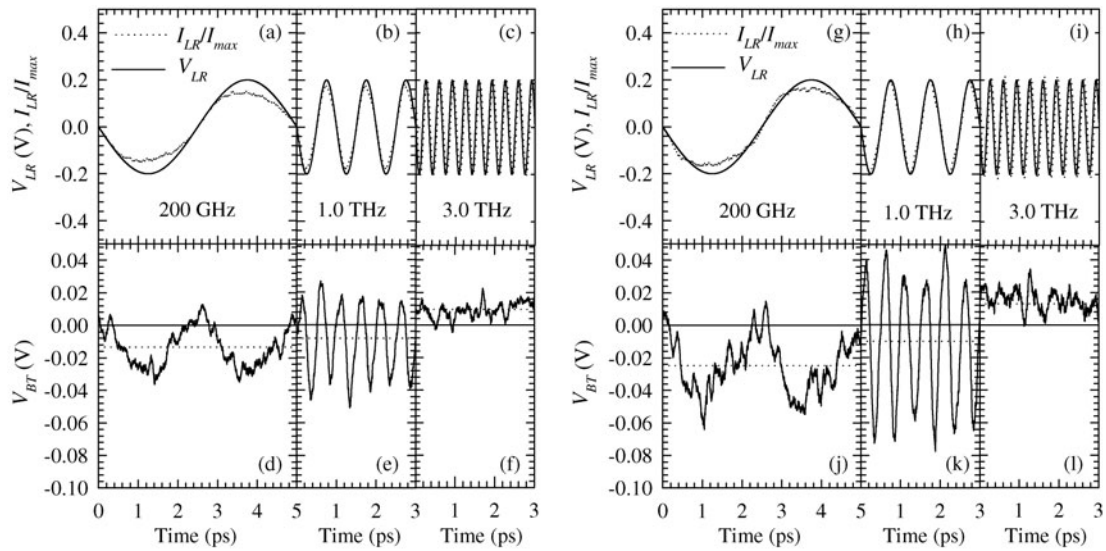


Figure 2. V_{BT} response to periodic signals with an amplitude of 0.2 V and frequencies of 200 GHz, 1.0 and 3.0 THz applied to V_{LR} (the potential difference between the left and right electrodes) in the ballistic rectifier of the inset of figure 1, at ((a)–(f)) 300 K and ((g)–(l)) 77 K. The dotted curves in (a)–(c) and (g)–(i) correspond to the normalized horizontal current, I_{LR}/I_{max} , and to the DC current level, $\overline{V_{BT}}$, in (d)–(f) and (j)–(l).

a non-zero V_{BT} , and since the trajectories of the electrons through the bottom and top branches (and also the times taken) are different, the resulting high frequency dependence of the response in the vertical potential difference is quite complicated. Therefore, the positive values of V_{BT} could be explained as a consequence of the different delays of the carrier redistributions in the top and bottom branches with respect to the applied voltage, that can lead, for some resonant frequencies, to inversion of the low frequency situation (higher concentration in the top branch).

To clarify this point, figure 3 presents the mean value of the response signal, $\overline{V_{BT}}$, as a function of the frequency of the applied AC signal (with the amplitude of 0.2 V) for different temperatures. For each temperature, the value of $\overline{V_{BT}}$ does not suffer important changes up to 0.5 THz. As seen before, $\overline{V_{BT}}$ has larger values for lower temperatures. Beyond this frequency, the efficiency of the rectification is reduced and the differences among the values of $\overline{V_{BT}}$ for the different temperatures are reduced. However, the rectification remains active up to 1.0 THz at room temperature. In figure 3 we also observe that in the high frequency range ($f > 1.5$ THz) the average response signal is positive, due to the impossibility of correct redistribution of the electronic concentration at such high frequencies. The frequency dependence of the rectifying effect is almost independent of temperature due to the transit times of the electrons being similar, since the motion in the horizontal direction is mainly limited by the geometry of the device (much more so than by the scattering mechanisms).

The dynamic response of the electron current can also be indicative of the ability of the electron concentration to react to an excitation. If the current does not respond to a high frequency of the applied $V_{LR}(t)$, a total loss in the response of $V_{BT}(t)$ will also take place. We will therefore study the dynamic current in the ballistic rectifier as another indicator of the global frequency response of the device. Figure 4(a) shows, at room temperature, the transient current response when,

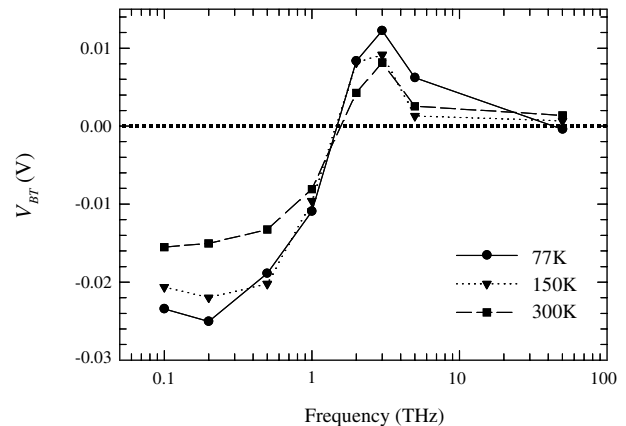


Figure 3. Mean value of the response signal, $\overline{V_{BT}}$, as a function of frequency of the periodic input AC signal with an amplitude of 0.2 V applied between the left and right electrodes for different temperatures.

starting from equilibrium conditions, a potential step of 0.05 V is applied between left and right electrodes. Note that after the voltage step, before reaching the new steady-state condition, an overshoot of the horizontal electron current takes place. Thus, at the corresponding frequencies, the transport inside the device and the electron concentration can show non-static effects, as positive values of the potential difference between the bottom and top electrodes. By Fourier transformation of the current shown in figure 4(a), the impedance of the devices as a function of the frequency can be obtained, figure 4(b). The real part of the impedance is frequency independent and its imaginary part is linear with the frequency. Thus, the small-signal equivalent circuit for the horizontal current is that presented in the inset of figure 4(b). It consists of a resistance of $1.36 \times 10^{-3} \Omega$ in series with a self-inductance of $3.29 \times 10^{-17} \text{ H m}$. Accordingly, the estimated cut-off frequency for the horizontal current at 300 K is 6.6 THz, a

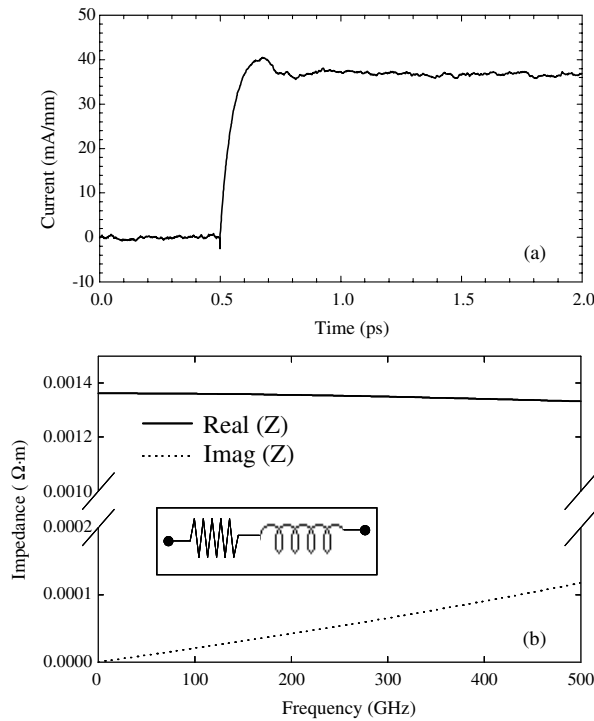


Figure 4. (a) Transient current through the device as a function of time when a voltage step of 0.05 V is applied between the left and right electrodes at 300 K and (b) the corresponding frequency dependent impedance. The inset shows the equivalent circuit for the current response of the ballistic rectifier at room temperature.

similar result to that of the previous study, but obtained in a simpler way. That means that the response of the potential difference in the vertical direction is connected to that of the horizontal current flux in the device, since both are closely related to the speed at which the electron concentration adapts to the input signal variations.

4. Conclusions

Using a Monte Carlo simulator, a semiclassical study of the dynamic behaviour of a InGaAs based ballistic rectifier has been performed. This device has exhibited an intrinsic cut-off frequency in the THz range, which is almost independent of temperature. The flexibility of our simulator for modelling any kind of geometry, very important in ballistic devices, makes it an excellent tool for the optimization of device performance with no need for technological processes.

Acknowledgments

This work was partially supported by the European Commission through the NANOTERA project IST-2001-32517, by the Dirección General de Investigación (Ministerio de Ciencia y Tecnología) and FEDER through the project TIC2001-1754 and by the Consejería de Educación y Cultura de la Junta de Castilla y León through the project SA057/02.

References

- [1] Hieke K and Ulfward M 2000 *Phys. Rev. B* **62** 16727
- [2] Shorubalko I, Xu H Q, Maximov I, Omling P, Samuelson L and Seifert W 2001 *Appl. Phys. Lett.* **79** 1384
- [3] Song A M, Lorke A, Kriele A, Kothaus J P, Wegscheider W and Bichler M 1998 *Phys. Rev. Lett.* **80** 3831
- [4] Song A M, Omling P, Samuelson L, Seifert W, Shorubalko I and Zirath H 2001 *Japan. J. Appl. Phys.* **40** L909
- [5] Mateos J, Vasallo B G, Pardo D, González T, Galloo J S, Bollaert S and Cappy A 2003 *Nanotechnology* **14** 117
- [6] Mateos J, Vasallo B G, Pardo D, González T, Galloo J S, Bollaert S and Cappy A 2003 *IEEE Trans. Electron Devices* **50** 1897
- [7] González T, Mateos J, Pardo D, Varani L and Reggiani L 1999 *Semicond. Sci. Technol.* **14** L37
- [8] Xu H Q 2001 *Appl. Phys. Lett.* **78** 2064
- [9] Worschech L, Xu H Q, Forchel A and Samuelson L 2001 *Appl. Phys. Lett.* **79** 3287